Available online at www.sciencedirect.com
SCIENCE DIRECT®
Journal of the European Ceramic Society 25 (2005) 3649–3655
www.elsevier.com/locate/jeurceramsoc

# Critical crack-healing condition for SiC whisker reinforced alumina under stress

Wataru Nakao*, Masato Ono, Sang-Kee Lee, Koji Takahashi, Kotoji Ando

*Department of Energy and Safety Engineering, Yokohama National University, 79-5 Tokiwadai, Hodogaya-ku, Yokohama 240-8501, Japan*

Received 11 April 2004; received in revised form 1 September 2004; accepted 12 September 2004
Available online 8 December 2004

**Abstract**

Alumina reinforced by SiC whisker, called here "alumina(w)" was developed with the objective of improving fracture toughness and crack-healing ability. The composites were crack-healed at 1200 °C for 8 h in air under elevated static and cyclic stresses. The bending strength at 1200 °C of the crack-healed composites were investigated. The threshold static stress during crack-healing of alumina(w) has been determined to be 250 MPa, and the threshold cyclic stress was found to be 300 MPa. Considering that the crack growth is time-dependent, the threshold stress of every condition during crack-healing of alumina(w) was found to be 250 MPa. The results showed that the threshold stress intensity factor during crack-healing was 3.8 MPa $m^{1/2}$. The same experiment conditions were applied to specimens cracked and annealed at 1300 °C for 1 h in Ar, to remove the tensile residual stress at a tip of the crack. Thus, the threshold stress intensity factor during crack-healing was found to be 3.2 MPa $m^{1/2}$ for the specimens crack-healed with annealing. The threshold stress intensity factor during crack-healing of alumina(w) was chosen to be 3.2 MPa $m^{1/2}$ to facilitate comparison with the values of the threshold stress intensity factor during crack-healing. The residual stress was slightly larger than the intrinsic value.


*Keywords:* Crack-healing; Composites; $Al_2O_3$; SiC whiskers

## 1. Introduction

Alumina ($Al_2O_3$) has three weak points:[1] (1) low bending strength ($\sigma_B \approx 400$ MPa), (2) low heat-resistance limit temperature for strength ($T_{HR} \approx 950$ °C), and (3) low fracture toughness ($K_{IC} \approx 4.0$ MPa $m^{1/2}$). These weaknesses restrict the application of $Al_2O_3$ for important components. If these weaknesses were satisfactorily overcome, $Al_2O_3$ would be a leading candidate material for advanced gas turbine and engine, because alumina exhibits much greater resistance to oxidation than silicon nitride.

For the weakness (1) above, the grain growth of $Al_2O_3$ during sintering was retarded and strength was increased by the Hall–Petch effect similar to mullite/SiC[2] by adding 15–20 mass% nanosize SiC particles. Considering item (2), Niihara and coworkers[3–6] have proposed the concept of "nanocomposite ceramics". Some $Al_2O_3$/SiC nanocomposites exhibit excellent strength and $T_{HR}$. The increased of $T_{HR}$, for alumina whose value is 1300 °C, was achieved by uniformly distributing nanosize SiC particles in alumina grains. Related to above weakness (3), two possibilities to overcome low fracture toughness are (a) increase in fracture toughness by reinforcing whiskers and fibers, and (b) endowing a strong self-crack-healing ability to heal the cracks. As to the above (b), monolithic $Al_2O_3$ and $Al_2O_3$/SiC composites have very interesting crack-healing ability.[1,7–15] That the crack-healing behavior of monolithic $Al_2O_3$ was induced not by intrinsic crack-healing but by the secondary sintering, is reported by the previous study.[1,13] By contrast, $Al_2O_3$/SiC composite has been crack-healed by reaction of SiC and the $O_2$ in the atmosphere. The crack-healing behavior of the previous $Al_2O_3$/SiC composite is assumed to be insufficient to overcome weakness (3) above. However, the good self-crack-healing ability was introduced as for mullite/SiC[2,16–20] and $Si_3N_4$/SiC[21–29] by adding 15–20 mass% nanosize SiC parti-

* Corresponding author.
*E-mail address:* wnakao@ynu.ac.jp (W. Nakao).

0955-2219/$ – see front matter © 2004 Elsevier Ltd. All rights reserved.
doi:10.1016/j.jeurceramsoc.2004.09.021

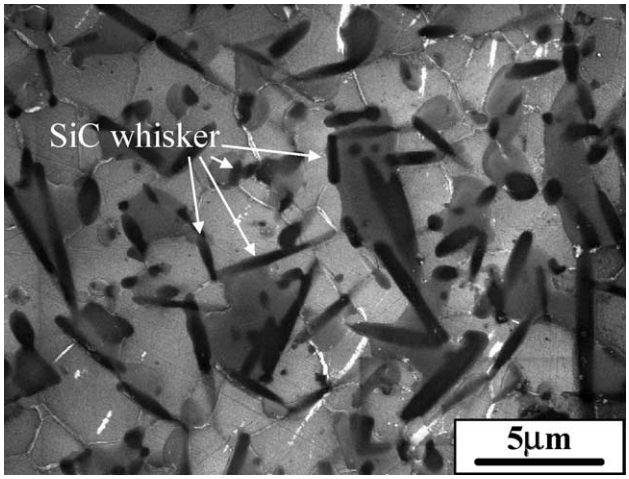


Fig. 1. Microstructure of the SiC reinforced alumina composite, alumina(w).

cles. However, oxygen is necessary for the crack-healing, so embedded flaws cannot be healed.

In conclusion, for higher structural integrity, both high fracture toughness and crack-healing ability should be satisfactorily achieved. From this perspective, alumina reinforced by 20 mass% SiC whisker, abbreviated alumina(w), was sintered and the mechanical properties of alumina(w) were investigated in the previous studies.[14,15] Alumina(w) exhibited large fracture toughness (6.5 MPa $m^{1/2}$) and excellent crack-healing ability. However, the basic crack-healing behavior as a function of crack-healing temperature and time was not well investigated. Moreover, crack-healing behavior under stress and the critical stress condition were not investigated at all. Therefore, alumina(w) has been subjected to crack-healing under elevated static and cyclic stresses at 1200 °C, corresponding to the limiting temperature for the bending strength of alumina(w). The bending strength of alumina(w) crack-healed under stress has been measured at the crack-healing temperature. From the results, an upper limiting stress that can be applied during crack-healing has been determined for alumina(w).

## 2. Experimental

The α-$Al_2O_3$ powder (AKP-20, Sumitomo Chemicals Co. Ltd., Japan) used in this study has a purity of 99.999% and a mean particle size of 0.4–0.6 μm. The SiC whiskers (SCW, Tateho Chemical Industry Co. Ltd., Japan) used have diameters between 0.8 and 1.0 μm and lengths from 30 to 100 μm. The mixture of α-$Al_2O_3$ powder and 20 mass% SiC whiskers was blended well in isopropyl alcohol for 12 h using alumina balls and an alumina mill pot. Then, the slurry was dried. Rectangular plates of 50 mm × 50 mm × 9 mm were sintered via uniaxial hot press in Ar at 1850 °C for 1 h at 40 MPa. Fig. 1 shows the microstructure of the sintered SiC whisker reinforced alumina composite, alumina(w). The grain size of α-$Al_2O_3$ was 5–6 μm. The SiC whiskers were located at grain boundaries between α-$Al_2O_3$ grains and were preferentially oriented within the plane perpendicular to the pressing axis. The density of the sintered plate was 3.83 g/$cm^3$. The sintered plate was cut into the 3 mm × 4 mm × 23 mm rectangular specimens bar that were polished to a mirror finish on one face and the edges of specimens were beveled 45° to reduce the likelihood of edge initiated failures.

A semi-elliptical surface crack of 100 μm in surface length, as shown in Fig. 2, was made at the center of the tensile surface of specimens with a Vickers indenter, using a load of 19.6 N. The aspect ratio (*a*/*c*) of the pre-crack which is depth (*a*) to half the surface length (*c*) was 0.9. In this investigation, the pre-crack was healed in air while applying tensile static or cyclic stresses by the three-point loading system shown in Fig. 3. The pre-crack was subjected to tensile stress before the crack-healing was started by heating the furnace to avoid the crack-healing under no-stress. Then, the specimen was kept at the above condition for 8 h to finish completely the crack-healing process. The applied cyclic stress was sinusoidal with a stress ratio, maximum stress/minimum stress, of 0.2 and a frequency of 5 Hz. Moreover, the crack-healing behavior under stress was also investigated for specimens annealed at 1300 °C for 1 h in Ar after pre-cracking so as to remove the residual stress introduced during pre-cracking by using the indentation method.

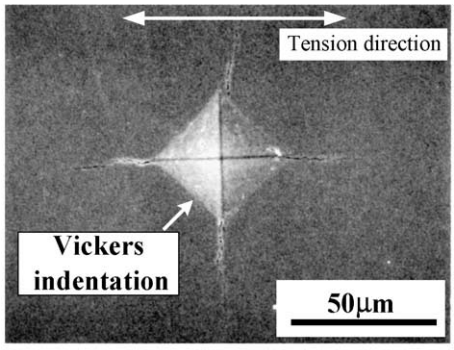


(a)

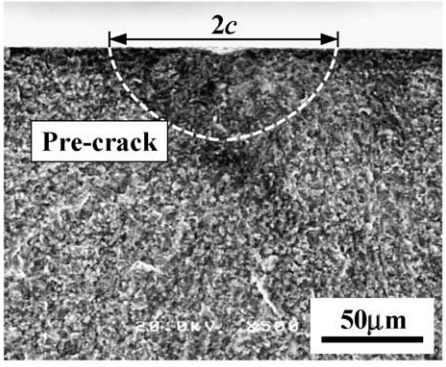


(b)

Fig. 2. SEM images of (a) surface shapes and (b) cross-sectional shapes of the crack and indentation.

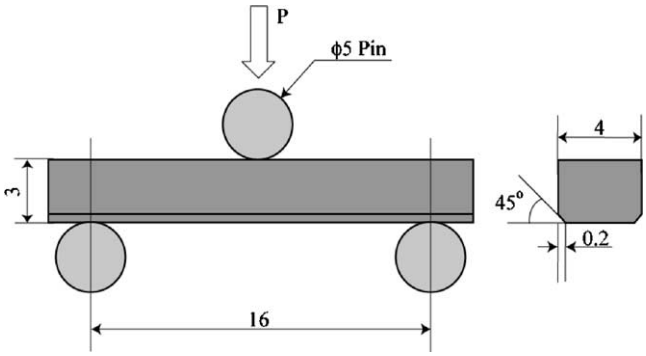


Fig. 3. Dimensions of the specimen and the three-point loading system used for this investigation.

All fracture tests of the specimens crack-healed were performed on a three-point loading system with a span of 16 mm at 1200 °C, corresponding to the crack-healing temperature. The cross-head speed in the monotonic test was 0.5 mm/min.

## 3. Result

In terms of basic knowledge, the crack-healing behavior of alumina(w) under no-stress[14,15] is now reviewed below. Fig. 4 shows the specimen surface crack-healed at 1300 °C for 2 h. The pre-crack after crack-healing cannot be observed in this figure. Fig. 5 shows the temperature dependence of the bending strength of the specimens crack-healed at 1300 °C for 2 h in air, with the room temperature bending strengths of the specimens as-received and as-cracked and the specimen without the pre-crack heat-treated at 1300 °C for 2 h in air so as to heal cracks introduced during machining. The bending strength of alumina(w) was reduced from 1000 to 500 MPa by cracking, and then that was recovered to the same strength as the as-received specimen by crack-healing at 1300 °C for 1 h. It is, therefore, confirmed that crack-healing is complete after holding the specimen at 1300 °C for 1 h. Moreover, the bending strength of the crack-healed specimen was slightly decreased by temperature increase from 400 to 1000 °C, but decreased with increasing temperature above 1000 °C. The specimens were fractured elastically below 1200 °C, and

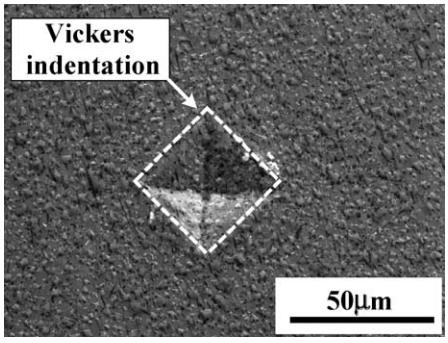


Fig. 4. Surface shapes of the crack and indentation crack-healed at 1300 °C for 2 h in air.

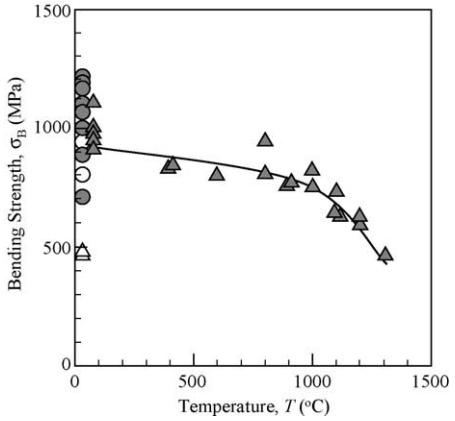


Fig. 5. Temperature dependence of the bending strength of the specimens crack-healed at 1300 °C for 2 h in air, with the room temperature bending strengths of the specimens as-received and as-cracked and the specimen without the pre-crack heat-treated at 1300 °C for 2 h in air so as to heal cracks introduced during machining. (▲) Crack-healed; (●) heat-treated; (△) as-cracked; (◯) as-received.

fractured with plastic deformation at 1300 °C. Thus, the limiting temperature for the bending strength of alumina(w) was determined to be 1200 °C.

Fig. 6 shows the relation between the applied stress during the crack-healing treatment for the specimens as-cracked and the bending strength at the crack-healing temperature of the specimens crack-healed under static and cyclic stress. The gray colored and open triangle indicate the bending strength of the specimen crack-healed under static stress, $\sigma_{ap,S}$, and cyclic stress, $\sigma_{ap,C}$, respectively, where the values of $\sigma_{ap,C}$ are the maximum of each applied cyclic stress. The bending strength of 0 MPa indicates the specimen fractured during crack-healing. Alumina(w) with the pre-crack of 100 μm were never fractured during crack-healing treatment under static stresses below 250 MPa, and the crack-healed specimen had the same bending strength as the specimens crack-healed

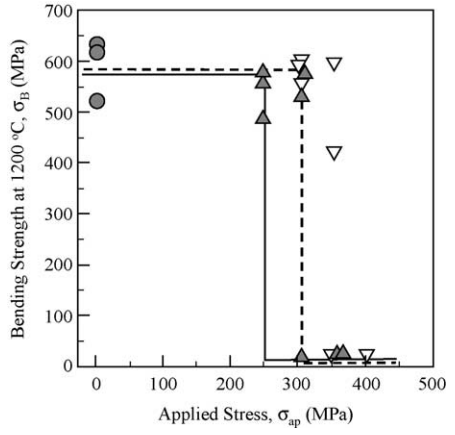


Fig. 6. Relation between the applied stress during the crack-healing treatment for the specimens as-cracked and the bending strength at the crack-healing temperature of the specimens crack-healed under static and cyclic stress. (▲) Crack-healed under static stress; (▽) crack-healed under cyclic stress; (●) crack-healed under no stress.

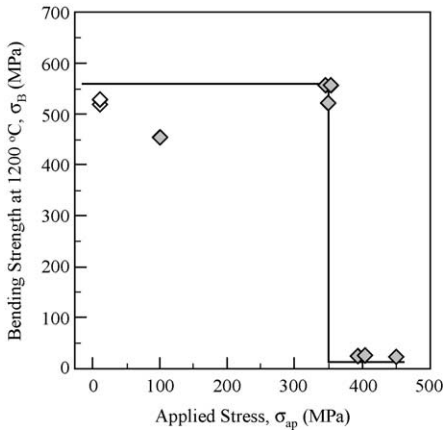


Fig. 7. Relation between the applied stress during the crack-healing treatment for the specimen annealed after pre-cracking and the bending strength at the crack-healing temperature of the specimens crack-healed under static stress. (◈) Crack-healed under static stress; (◊) crack-healed under no stress.

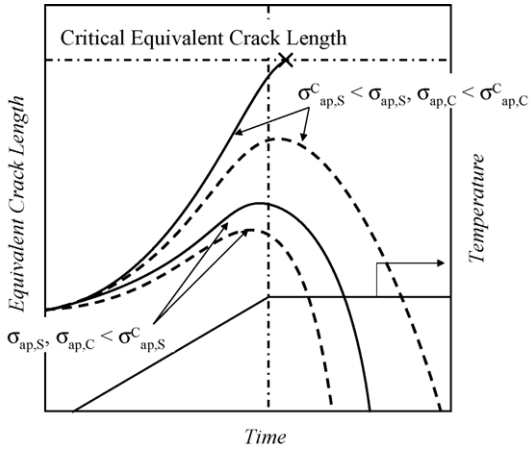


Fig. 8. Schematic diagram of the crack growth and healing behavior during the crack-healing under stress. (—) Crack-healed under static stress; (- - -) crack-healing under cyclic stress.

under no-stress at 1200 °C. Crack-healing under static stress of 300 MPa, a few cracked specimens were fractured during the crack-healing treatment. All cracked specimens were fractured during crack-healing under static stress of 350 MPa. Therefore, the threshold static stress during crack-healing of alumina(w) having the pre-crack, $\sigma^{C}_{ap,S}$, was found to be 250 MPa, where the threshold stress during crack-healing is defined as the upper stress limit not to fracture the specimen during crack-healing. Also, the threshold cyclic stress, $\sigma^{C}_{ap,S}$, was found to be 300 MPa. The details of the reason for $\sigma^{C}_{ap,S}$ being smaller than $\sigma^{C}_{ap,C}$ are discussed in Section 4.

Fig. 7 shows the relation between the applied stress during the crack-healing treatment for the specimen annealed after pre-cracking and the bending strength at the crack-healing temperature of the specimens crack-healed under static stress. From this figure, the threshold stress during crack-healing was found to be 350 MPa.

## 4. Discussion

### 4.1. Mechanism of crack growth and crack-healing

Fig. 8 shows the schematic diagram of the crack growth and healing behavior during the crack-healing under stress. The solid lines indicate the equivalent crack length change during the crack-healing under static stress. Also the dash lines indicate it under cyclic stress. The driving force for crack growth, which is called the "crack driving force" by Irwin,[30] increases with increasing applied stress and crack length. Thus, the crack growth rate increased with increasing the time applied stress to the crack. On the other hand, the driving force for crack-healing, called for short "crack-healing force"[17,31] is not affected by the applied stress. The crack-healing rate increased simply with the temperature increasing. Crack-healing starts preventing crack growth above the temperature that the crack-healing rate becomes non-negligible compared with the crack growth rate. Moreover, the crack starts healing when the crack-healing rate becomes larger than the crack growth rate. The threshold stress imposes an upper limit to the crack growth rate thereby limiting the crack length to less than the critical crack length before crack-healing starts. From a comparison with the values of $\sigma^{C}_{ap,S}$ and $\sigma^{C}_{ap,C}$, it may be confirmed that the crack growth behavior of alumina(w) is time dependent rather than cyclic dependent. It is, therefore, concluded that applying static stress is the most fracturable condition for crack-healing behavior under stress and that the threshold stresses of every condition during crack-healing of alumina(w), $\sigma^{C}_{HS}$, has been determined to be 250 MPa.

### 4.2. Stress intensity factor of the stress limiting during crack-healing treatment

The stress intensity factor for the tip of the pre-crack during the crack-healing treatment, $K_{HS}$, was estimated. Since a tensional residual stress was introduced during pre-cracking by using the indentation method, it is necessary for the estimation to consider the stress intensity factor of the residual stress, $K_R$, as expressed by the following equation:

$$K_{HS} = K_{ap} + K_R \quad (1)$$

where $K_{ap}$ is evaluated by Newman–Raju equation[32] using the stress applying during the crack-healing treatment, $\sigma_{ap}$. Moreover, ceramics having small flow show non-linear fracture mechanics. Therefore, the residual stress was evaluated by the following procedure.

The stress intensity factor of the residual stress, $K_R$, was evaluated by subtracting the critical stress intensity factor of the specimen as cracked, $K_M$, from the value of the specimen cracked and annealed at 1300 °C for 1 h in Ar to remove the

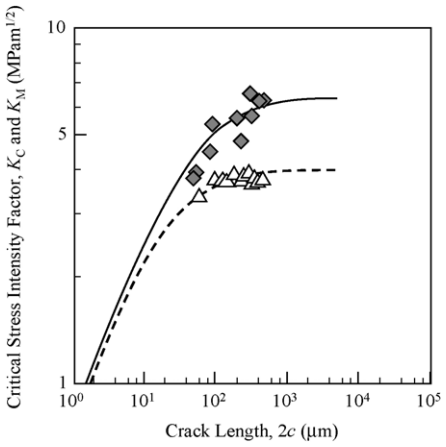


Fig. 9. Critical stress intensity factors, $K_C$ and $K_M$, as a function of surface length of pre-crack, 2$c$, for the specimen as-cracked and annealed after pre-cracking. (△) As-cracked; (◇) annealed after pre-cracking.

residual stress, $K_C$:

$$K_R = K_C - K_M \tag{2}$$

In the previous study[15], the bending strength of the specimens as-cracked and annealed after pre-cracking, $\sigma_M$ and $\sigma_C$, had been measured. From the results, the critical stress intensity factors, $K_C$ and $K_M$, were evaluated by the Newman–Raju equation. Fig. 9 shows the $K_C$ and $K_M$ as a function of 2$c$, where the gray colored diamond and open triangles indicate the values of $K_C$ and $K_M$, respectively. The difference between $K_C$ and $K_M$ indicates $K_R$. The crack size dependence of $K_R$ can be obtained by determining the formula between crack size and $K_M$ or $K_C$. One of the present authors[33–35] has proposed non-linear fracture mechanics for engineering ceramics by using process zone size, as shown in Eq. (3):

$$\begin{cases} D_C = \dfrac{\pi}{8}\left(\dfrac{K_{IC}}{\sigma_o}\right)^2 = a_e\left\{\sec\left(\dfrac{\pi\sigma_C}{2\sigma_o}\right) - 1\right\} \\ D_C = \dfrac{\pi}{8}\left(\dfrac{K_{IM}}{\sigma_o}\right)^2 = a_e\left\{\sec\left(\dfrac{\pi\sigma_M}{2\sigma_o}\right) - 1\right\} \end{cases} \tag{3}$$

where $D_C$ is size limit of the process zone and $\sigma_o$ is the stress forming the process zone, corresponding to the fracture strength of the plain specimen. The equivalent crack length, $a_e$, was evaluated from the stress intensity factor by using the Newman–Raju equation. Assuming $a/c = 0.9$, $a/H \ll 1$ and $c/B \ll 1$, the relation between surface length of the pre-crack and $a_e$ was expressed by:

$$a_e = 0.236\,(2c) \tag{4}$$

Moreover, the critical stress intensity factors, $K_C$ and $K_M$, were obtained from Eq. (5) using $\sigma_C$, $\sigma_M$ and $a_e$:

$$K_C = \sigma_C(\pi a_e)^{1/2}, \qquad K_M = \sigma_M(\pi a_e)^{1/2} \tag{5}$$

Introducing Eqs. (4) and (5) to Eq. (3), the stress intensity factors of the fracture conditions, $K_C$ or $K_M$, related with the equivalent crack length, 2$c$, according Eq. (6):

$$\begin{cases} D_C = \dfrac{\pi}{8}\left(\dfrac{K_{IC}}{\sigma_o}\right)^2 \\ \quad = 0.236 \times 2c\left[\sec\left\{\dfrac{K_C}{2\sigma_o}\left(\dfrac{\pi}{0.236 \times 2c}\right)^{1/2}\right\} - 1\right] \\ D_C = \dfrac{\pi}{8}\left(\dfrac{K_{IM}}{\sigma_o}\right)^2 \\ \quad = 0.236 \times 2c\left[\sec\left\{\dfrac{K_M}{2\sigma_o}\left(\dfrac{\pi}{0.236 \times 2c}\right)^{1/2}\right\} - 1\right] \end{cases} \tag{6}$$

Each data set of $K_C$ and $K_M$ was subjected to the least square fitting by using Eq. (6). Both curves are approximately constant at crack lengths above $10^3$ μm, and the values of $K_{IC}$ and $K_{IM}$, corresponding to the constant values in Fig. 9, were determined to be 6.5 and 4.0 MPa m$^{1/2}$, respectively. From the obtained values, the stress intensity factor of the tensional residual stress resulting from the introduction of a pre-crack of $2c = 100$ μm was determined to be 1.6 MPa m$^{1/2}$.

By adding the obtained value of $K_R$, it is possible to calculate the value of $K_{HS}$ for the specimen as-cracked from Eq. (1). On the other hand, $K_{HS}$ for the specimen annealed after pre-cracking was equal to $K_{ap}$. Fig. 10 shows the relation between the $K_{HS}$ for the specimens as-cracked and annealed after pre-cracking and the bending strength at the crack-healing temperature of the specimens crack-healed under static stress. The gray colored triangle and the open diamond indicate the results for the specimens as-cracked and annealed after pre-cracking, respectively. The threshold stress intensity factors during crack-healing, $K_{HS}^C$, have been determined to be 3.8 and 3.2 MPa m$^{1/2}$ for the specimens crack-healed without annealing and with annealing, respectively. From a comparison with the values of the threshold stress intensity factor during crack-healing, the residual stress is evaluated slightly larger than the intrinsic

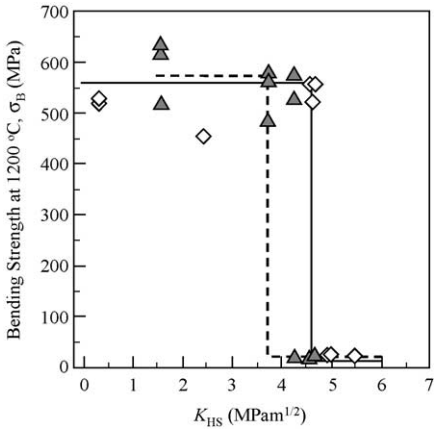


Fig. 10. Relation between the $K_{HS}$ for the specimens as-cracked and annealed after pre-cracking and the bending strength at the crack-healing temperature of the specimens crack-healed under static stress. (▲) As-cracked; (◊) annealed after pre-cracking.

value. Therefore, the threshold stress intensity factor during crack-healing of alumina(w) is selected as 3.2 MPa $m^{1/2}$. It is, however, confirmed that both values did not differ greatly although the applied stress changes by 50 MPa.

## 5. Conclusion

Alumina reinforced by SiC whisker, alumina(w) was developed with the objective of improving fracture toughness and crack-healing ability. The composites were crack-healed at 1200 °C for 8 h in air under elevated static and cyclic stresses and the bending strength at 1200 °C of the crack-healed composites were then investigated. Alumina(w) with the pre-crack of 100 μm were never fractured during crack-healing treatment under static stresses below 250 MPa, and the crack-healed specimen had the same bending strength as the specimens crack-healed under no-stress at 1200 °C. Therefore, the threshold static stress during crack-healing of alumina(w) was found to be 250 MPa. Also, the threshold cyclic stress was found to be 300 MPa. Considering that the crack growth is time-dependent, the threshold stress of every condition during crack-healing of alumina(w) has been concluded to be 250 MPa. Moreover, the same experiment is conducted on specimens annealed at 1300 °C for 1 h in Ar after pre-cracking. Thus, the threshold static stress during crack-healing of alumina(w) annealed after pre-cracking has been determined to be 350 MPa. From the results, the threshold stress intensity factor during crack-healing has been evaluated as 3.8 and 3.2 MPa $m^{1/2}$ for the specimens crack-healed without annealing and with annealing, respectively. A comparison with the values of the threshold stress intensity factor during crack-healing shows that the residual stress is slightly larger than the intrinsic value. Therefore, the threshold stress intensity factor during crack-healing of alumina(w) is selected as 3.2 MPa $m^{1/2}$.

## References


1. Kim, B. S., Ando, K., Chu, M. C. and Saito, S., Crack-healing behavior of monolithic alumina and strength of crack-healed member. *J. Soc. Mat. Sci. Jpn.*, 2003, **52**, 667–673.
2. Chu, M. C., Sato, S., Kobayashi, Y. and Ando, K., Damage healing and strengthealing behavior in intelligent mullite/SiC ceramics. *Fatigue Fract. Eng. Mater. Struct.*, 1995, **18**, 1019–1029.
3. Niihara, K. and Nakahira, A., Strengthening of oxide ceramics by SiC and $Si_3N_4$ dispersions. In *Proceedings of the Third International Symposium on Ceramic Materials and Components for Engines*, 1988, pp. 919–926.
4. Niihara, K., New design concept of structural ceramics—ceramics nanocomposite. *J. Ceram. Soc. Jpn.*, 1991, **99**, 974.
5. Ohji, T., Nakahara, A., Hirano, T. and Niihara, K., Tensile creep behavior of alumina/silicon carbide nanocomposite. *J. Am. Ceram. Soc.*, 1994, **77**, 3259–3562.
6. Jeong, Y. K., Nakahira, A. and Niihara, K., Effects of additives on microstructure and properties of alumina–silicon carbide nanocomposites. *J. Am. Ceram. Soc.*, 1999, **82**, 3609–3612.
7. Moffatt, J. E., Plumbridge, W. J. and Hermann, R., High temperature crack annealing effect on fracture toughness of alumina and alumina–SiC composite. *Br. Ceram. Trans.*, 1996, **95**, 23–29.
8. Gupta, T. K., Crack healing and strengthening of thermally shocked alumina. *J. Am. Ceram. Soc.*, 1976, **59**, 259–262.
9. Mitomo, M., Nishihara, T. and Tsutsumi, M., Crack healing in silicon nitride and alumina ceramics. *J. Mater. Sci. Lett.*, 1996, **15**, 1976–1978.
10. Kim, H. E. and Moorhead, A. J., Oxidation behaviour and effects of oxidation on the strength of SiC-whisker reinforced alumina. *J. Mater. Sci.*, 1994, **29**, 1656–1661.
11. Chou, I. A., Chan, H. M. and Harmer, M. P., Effect of annealing environment on the crack healing and mechanical behavior of silicon carbide-reinforced alumina nanocomposites. *J. Am. Ceram. Soc.*, 1998, **81**, 1203–1208.
12. Deng, Z. Y., Shi, J. L., Zhang, Y. F., Lai, T. R. and Guo, J. K., Creep and creep-recovery behavior in silicon-carbide-particle-reinforced alumina. *J. Am. Ceram. Soc.*, 1999, **82**, 944–952.
13. Ando, K., Kim, B. S., Kodama, S., Ryu, S. H., Takahashi, K. and Saito, S., Fatigue strength of an $Al_2O_3$/SiC composite and a monolithic $Al_2O_3$ subjected to crack-healing treatment. *J. Soc. Mat. Sci. Jpn.*, 2003, **52**, 1464–1470.
14. Takahashi, K., Yokouchi, M., Lee, S. K. and Ando, K., Crack-healing behavior of $Al_2O_3$ toughened by SiC whiskers. *J. Am. Ceram. Soc.*, 2003, **86**, 2143–2147.
15. Ando, K., Yokouchi, M., Lee, S. K., Takahashi, K., Nakao, W. and Suenaga, H., Crack-healing behavior, high temperature strength and fracture toughness of alumina reinforced by SiC whiskers. *J. Soc. Mat. Sci. Jpn.*, 2004, **53**, 599–606.
16. Ando, K., Tuji, K., Furusawa, K., Hanagata, T., Chu, M. C. and Sato, S., Effect of pre-crack size and testing temperature on fracture strength properties of crack healed mullite. *J. Soc. Mat. Sci. Jpn.*, 2001, **50**, 920–925.
17. Ando, K., Furusawa, K., Chu, M. C., Hanagata, T., Tuji, K. and Sato, S., Crack healing behavior under stress of mullite/silicon carbide ceramics and the resultant fatigue strength. *J. Am. Ceram. Soc.*, 2001, **84**, 2073–2078.
18. Ando, K., Chu, M. C., Tuji, K., Hirasawa, T., Kobayashi, Y. and Sato, S., Crack healing behaviour and high-temperature strength of mullite/SiC composite ceramics. *J. Eur. Ceram. Soc.*, 2002, **22**, 1313–1319.
19. Ando, K., Tsuji, K., Nakatani, M., Chu, M. C., Sato, S. and Kobayashi, Y., Effects of $Y_2O_3$ on crack healing temperature strength of structural mullite. *J. Soc. Mat. Sci. Jpn.*, 2002, **51**, 458–464.
20. Ono, M., Ishida, W., Nakao, W., Ando, K., Mori, S. and Yokouchi, M., Crack-healing behavior, high temperature strength and fracture toughness of mullite/SiC whisker composite ceramic. *J. Soc. Mat. Sci. Jpn.*, in press.
21. Ando, K., Ikeda, T., Sato, S., Yao, F. and Kobayashi, Y., A preliminary study on crack healing behavior of $Si_3N_4$/SiC composite ceramics. *Fatigue Fract. Eng. Mater. Struct.*, 1998, **21**, 119–122.
22. Chu, M. C., Ando, K., Sato, S., Hirasawa, T. and Kobayashi, Y., Crack-healing behavior of silicon nitride ceramics (effect of chemical composition on crack healing ability). *High Pressure Inst. Jpn.*, 1998, **36**, 82–89.
23. Ando, K., Chu, M. C., Kobayashi, Y., Yao, F. and Sato, S., The study on crack healing behavior of silicon nitride ceramics. *Jpn. Soc. Mech. Eng.*, 1998, **64 A**, 1936–1942.
24. Ando, K., Chu, M. C., Kobayashi, Y., Yao, F. and Sato, S., Crack healing behavior and high temperature strength of silicon nitride ceramics. *Jpn. Soc. Mech. Eng.*, 1999, **65 A**, 1132–1139.
25. Yao, F., Ando, K., Chu, M. C. and Sato, S., Static cyclic fatigue behaviour of crack-healed $Si_3N_4$/SiC composite ceramics. *J. Eur. Ceram. Soc.*, 2001, **21**, 991–997.
26. Ando, K., Houjou, K., Chu, M. C., Takeshita, S., Takahashi, K., Sakamoto, S. *et al.*, Crack-healing behavior of $Si_3N_4$/SiC ceramics under stress and fatigue strength at the temperature of healing (1000 °C). *J. Eur. Ceram. Soc.*, 2002, **22**, 1339–1346.

27. Houjou, K., Hirai, K., Ando, K., Chu, M. C., Matushita, S. and Sato, S., Effect of sintering additives and SiC on high temperature oxidation behavior of silicon nitride. *J. Soc. Mat. Sci. Jpn.*, 2002, **51**, 1235–1241.
28. Takahashi, K., Kim, B. S., Chu, M. C., Sato, S. and Ando, K., Self crack-healing behavior under stress of silicon nitride ceramics and resultant strength at the crack-healing temperature. *Jpn. Soc. Mech. Eng.*, 2002, **68**, 1063–1070.
29. Ando, K., Takahashi, K., Nakayama, S. and Sato, S., Crack-healing behavior of $Si_3N_4$/SiC ceramics under cyclic stress and resultant strength at the crack-healing temperature. *J. Am. Ceram. Soc.*, 2002, **85**, 2268–2272.
30. Irwin, G. A., Analysis of stresses and strains nears the end of a crack traversing a plate. *Trans. ASME J. Appl. Mech.*, 1957, **24**, 361–364.
31. Ando, K., Chu, M. C., Yao, F. and Sato, S., Fatigue strength of crack healed $Si_3N_4$/SiC composite ceramics. *Fatigue Fract. Eng. Mater. Struct.*, 1999, **22**, 897–903.
32. Newman, J. C. and Raju, I. S., An empirical stress-intensity factor equation for the subsurface crack. *Eng. Fract. Mech.*, 1981, **15**, 185–192.
33. Ando, K., Iwasa, M., Kim, B. A., Chu, M. C. and Sato, S., Effect of crack length, notch root radius and grain size of fracture toughness of fine ceramics. *Fatigue Fract. Eng. Mater. Struct.*, 1993, **16**, 995–1006.
34. Chu, M. C. and Ando, K., A fracture and severity analysis of composite ceramics. *Fatigue Fract. Eng. Mater. Struct.*, 1993, **16**, 335–350.
35. Tuji, K., Iwasa, K. and Ando, K., The location of crack initiation sites in alumina, polycarbonate and mild steel. *Fatigue Fract. Eng. Mater. Struct.*, 1999, **22**, 509–517.